Regular Article

Catalytic Decomposition of Methane and Ethylene into the Carbon and Hydrogen

S.H. Mousavipour*, M.M. Doroodmand, S. Amini and M. Shahamat

Department of Chemistry, College of Science, Shiraz University, Shiraz, 71454, Iran

(Received 29 July 2014, Accepted 30 November 2014)

The role of nickel as catalyst on the conversion of methane and ethylene in a gas phase flow reactor in the absence of oxygen is studied. In this study, nickel in its different forms is used as catalyst. The role of pressure, flow rate, and temperature on the conversion of feed gases is investigated. The experiments have been carried out in the presence and absence of the catalysts to measure the efficiency of the catalyst activity towards the conversion of the feed gases. Major products have been found to be carbon as soot or coke and hydrogen when methane is used as feed gas. Up to 97% conversion of the ethylene to methane, ethane, hydrogen, and carbon soot were achieved on the surface of the honeycomb nickel catalyst at 900 ± 10 K and 415 ± 5 Torr pressure, while the conversion of methane to hydrogen and carbon on the surface of NiO/SiO_2 catalyst was found to be up to 36% at 930 ± 10 K and 490 ± 5 Torr pressure with no sign of C_2 or C_3 formation. The carbon buildup on the surface of the prepared catalysts is also investigated.

Keywords: Nickel catalyst, Methane, Ethylene, Hydrogen formation

INTRODUCTION

One of the major troubles caused by the activity of human beings in modern societies is increasing the rate of global warming that can be linked to emission of greenhouse gases into the atmosphere [1]. Many attempts have been made to reduce this rate. One of the optimistic options being explored for the reduction of anthropogenic greenhouse gases emission is using hydrogen as a fuel instead of gasoline or natural gas [2]. Natural gas is a fossil fuel which is more suitable as raw material for alternative energy generation.

Molecular hydrogen is widely used in fuel cells, which directly converts the chemical energy in molecular hydrogen to electricity, with pure water and potentially useful heat as the only byproducts. Nowadays, molecular hydrogen is widely used in petroleum industry, ammonia production, hydrogenation of fats, oil field welding, hydrochloric acid production, rockets fuel, besides its usage in fuel cells to produce clean energy. Hydrogen has the

potential to run a fuel-cell engine with greater efficiency over an internal combustion engine. The same amount of hydrogen will take a fuel-cell car at least twice as far as a car running on gasoline [3]. Different methods for methane conversion, which is the main constituent of the natural gas, are being explored and suggested to overcome the atmospheric pollution crisis, while the economic issue is one of the major concerns.

Hydrogen does not occur free in nature in useful quantities. There are two main methods to produce hydrogen, electrolysis of water or hydrocarbon reforming. Conversion of hydrocarbons to produce hydrogen is one of the subjects that received much attention for environmental and industrial aspects. One of the efficient techniques for hydrocarbon reforming process is using different kinds of catalysts besides other methods like electrical spark or arc discharge. Electrical direct or alternative current spark or arc discharge techniques are other methods for conversion of natural gas (mainly methane) into the heavier hydrocarbons, carbon, and molecular hydrogen that has been proven to be less expensive [4].

About 50 percent of the word's hydrogen is extracted

___
*Corresponding author. E-mail: mousavi@susc.ac.ir

from natural gas, with ~40 percent coming from steam reforming of methane (CH_4) that its cost is relatively high beside formation of a lot of CO and CO_2 [5]. One of the major problems in steam reforming of methane is its high thermodynamic potential to coke formation [6]. A routine method for the fabrication of the synthesis gas is the partial oxidation of CH_4 by both O_2 or CO_2 [7,8,9]. However, in CO_2 reforming of CH_4, the deactivation of the catalyst by coke formation reserves a great challenge in development of a practical catalyst.

Another trouble in natural gas conversion in the presence of a catalyst is the undesirable carbon deposition in the filament forms, which have high mechanical strength and the catalyst particle is destroyed when the filaments hit the pore walls. This process may result in increasing pressure drop and hot tubes [10]. The resistance of nickel catalysts to coking can be increased by modifying the type of the support [11], or introducing some promoters and additives such as small amount of sulfur [12] or alkali [13] as well as rare earth oxides [14] or MoO_3, [15] that seems to be effective in preventing coke formation. However, the application of these promoters causes, in most of the cases, a considerable decrease in the specific activity of nickel catalyst.

Catalyst development has played a crucial role in the advances that have occurred; nevertheless, there remains a need for catalysts that promote higher selectivity to the desired product and have a longer life time. It has been proven that some of the transition metals can be used as effective catalysts for such purposes [16]. Noble metals could be used as catalysts for the conversion of methane to hydrogen and carbon in different forms [17]. The catalysts based on noble metals are reported to be less sensitive to coking compared to nickel based catalysts [18,19]. However, the fact that these noble metals are expensive and of limited availability makes the development of active and stable catalysts as these kind a challenge to the catalytic scientific community. Nickel in its different forms is used as an effective heterogeneous catalyst in various industries like dehydrogenation of light hydrocarbons.

Normally it is possible to reach to more than 98% conversion of methane in the steam reforming process [20]. The problem with this method is the formation of CO or CO_2 during the reaction.

Muradov [21] reported 70% conversion of methane on the surface of carbon at 1123 K. Zhang and co-workers [22] reported a CH_4 conversion of 23% on the surface of W,Zn/H-ZSM-5 catalyst at 1123 K with high benzene selectivity [23]. In a recycle flow rate of 120 ml min^{-1} on the surface of Pd/Al_2O_3 and in the presence of O_2, Lunsford reached to 25 ml min^{-1} conversion of methane. Couttenye *et al*. [24] studied the effect of temperature on the methane conversion on the surface of Ni and NiO. They reported 45% of methane conversion in a flow rate of 30 ml min^{-1} at 823 K. Mass spectroscopy data showed 100% selectivity toward hydrogen in the gas phase for methane decomposition on the surface of nickel catalyst. No detrimental effect on the activity or selectivity was observed after 25 h of continuous operation. Hu *et al*. [7] reached to 21% conversion on the surface of Ca-Ni/TiO_2 at 1050 K, while Monnerat *et al*. [25] reached to %45 methane conversion in a 4.67 mol m^{-3} concentration of methane on the surface of nickel gauze at 773 K [26]. On the surface of Ni/SiO_2 catalyst with 15% Ni, Aiello *et al*. reached to 30% of methane conversion at 923 K in a successive cracking cycles.

In this study three different forms of nickel as catalyst have been adopted to measure their activities towards the conversion of methane (the major compartment of the natural gas) and ethylene (another compartment of the natural gas) and also the durability of the most effective catalyst which is investigated in this study. The purpose of measuring the ethylene conversion on the surface of catalysts in this study is just its presence in the natural gas stream.

EXPERIMENTAL

Reagents and Analytical Techniques

Three different forms of nickel were used as catalyst in this study. The honeycomb form of metallic nickel supplied from Nano Pooshesh Felez Company [27] which was used as it was received. Sol-gel method was used to synthesize supported nickel oxide on silicon oxide as catalyst. The nano-scale nickel catalyst deposited on the surface of zeolite particles using mixed matrix membranes (MMMs) as interface was another form of nickel catalyst which was used in this study. The physical and chemical structures of

the prepared catalysts were characterized by X-ray diffraction (XRD), Fourier transform infrared (FTIR), scanning electron microscopy (SEM), Brunauer-Emmett-Teller (BET) method [28] for specific surface area determination, Barrett-Joyner-Halenda (BJH) method [29] for determination of mean pore diameter on the surface of the synthesized catalysts, and inductively coupling plasma (ICP) techniques to measure the amount of nickel in prepared catalysts. A gas flow reactor was used to investigate the efficiency of the prepared catalysts on the conversion of methane or ethylene.

Preparation and Characterization of Catalysts

Sol-gel method was used to prepare silicon oxide as supporting material for nickel oxide. The standard method was used to synthesize the sol gel [30,31]. The silica sol was prepared in a two-stage process. In the first stage, $Si(OC_2H_5)_4$ (TEOS), NH_4OH and C_2H_5OH in a specified volume ratio were mixed at room temperature and added into a solution of $NiCl_2$ and ethylene glycol. The prepared solution was refluxed for 5 h. Then TEOS, water, and glycerol with volume ratio of 6:12: 2 were added to the refluxed solution to form the sol at pH~9. The prepared sol was aged at 40 °C for 7 days and then was heated at 190 °C for 12 h. Formation of a gray-black turbidity suspension was an indication of $Ni(OH)_2$ or NiO formation on the surface of SiO_2. The powder was washed out and filtered three times with distilled water. Final washing was then accomplished by the pure acetone at room temperature and at last heated for 40 min at 600 °C. Analyzing techniques such as XRD, IR, SEM, BET, BJH, and ICP were used to characterize the physical and chemical properties of the prepared catalyst. Figure 1 shows the SEM images of the synthesized catalyst NiO/SiO_2. The white spot parts in the images are the indication of formation of the nickel oxide. The analytical results indicate the high percentage conversion of supported nickel hydroxide into the nickel oxide. In Fig. 2, the FTIR spectra of SiO_2 and NiO/SiO_2 are shown. The sharp peak at 3790 cm^{-1} is assigned to the stretching vibrational mode (vOH) of non-hydrogen bonded hydroxyl groups in the nickel hydroxide, while the broad band at 3547 cm^{-1} is assigned to the stretching mode of hydrogen bonded hydroxyl groups in the same layered structure. The absorption band in the regions between 750-
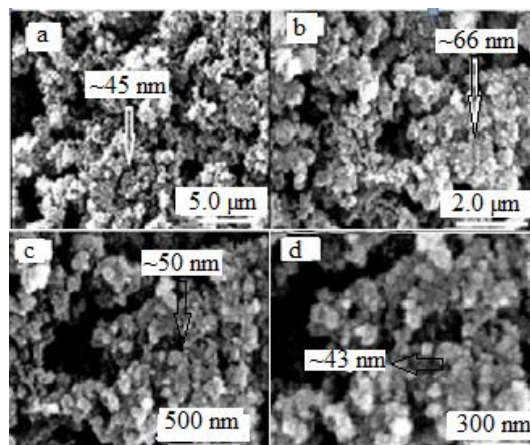

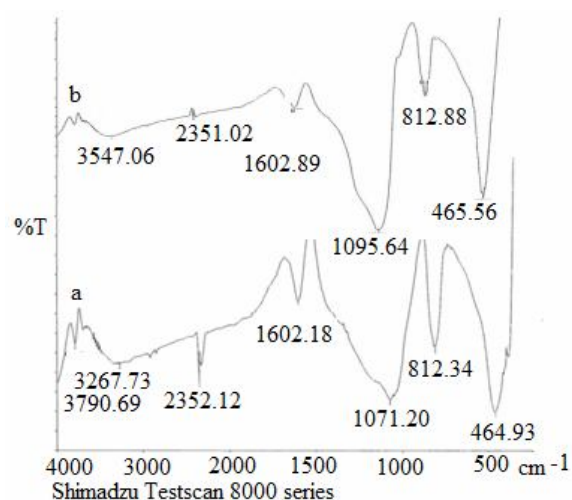**Fig. 1.** SEM images of the outer surface of synthesized NiO/SiO_2 catalyst.

Fig. 2. FTIR spectra of the silica samples including unsupported silica particles (a) and nickel-supported silica particles after heat treatment (b).

850 cm^{-1} is assigned to the Ni-O-H vibration bond. In the same region (800 to 820 cm^{-1}) the absorption band for the vibration of Si-O-Si is observed. The absorption at 460 to 490 cm^{-1} assigned to the stretching vibration of Ni-OH [32]. A weak band near 1600 cm^{-1}, assigned to H-O-H bending vibration modes, was also presented due to the adsorption of water in air when FTIR sample disks were prepared in an open air [33]. The absorption band in the regions between

48

1000-1200 cm^{-1} is attributed to SiO_2 stretching modes [34]. The XRD pattern of SiO_2 and NiO/SiO_2 is shown in Fig. 3. The silicon X-ray pattern is compatible with the pattern reported in reference [35]. The XRD patterns for NiO/SiO_2 and $Ni(OH)_2$ are compatible with the patterns reported by Bahari *et al*. [36] and Saghatforoush *et al*. [37]. As clearly shown, the NiO nanoparticles have been immobilized on the SiO_2 as support. This spectroscopic technique is considered as an acceptable proof for the capability of the recommended procedure for direct immobilization of NiO nanostructures on a solid matrix such as SiO_2.

The specific surface area (SSA) of the NiO/SiO_2 catalysts is measured by N_2 adsorption using BET isotherm. In this method the adsorption and desorption of N_2 on the surface of the catalyst at 77 K is measured to find the BET isotherm constants. According to the BET results, the SSA for prepared samples of NiO/SiO_2 was found to be in a range of 221 to 273.8 m^2 g^{-1} from the different prepared samples. The BJH method is used to measure the mean pore diameter of the synthesized catalysts. The Mean pore diameter of synthesized NiO/SiO_2 catalyst was found to be 8.02 nm. The isotherms indicate a mesopores structure for the prepared catalyst. The synthesized NiO/SiO_2 catalyst was analyzed by the ICP to measure the amount of nickel in the prepared catalyst. The results indicate the amount of nickel in the catalyst is close to 4.5 to 5 weight percent.

Another form of the catalyst that was used in this study was nickel coated on the surface of zeolite grains. Zeolite 3A is a crystalline molecular sieve and highly porous material which belongs to the class of aluminosilicates. These crystals are characterized by a three-dimensional pore system, with pores of precisely defined diameter. The corresponding crystallographic structure is formed by tetrahedrons of (AlO_4) and (SiO_4). These tetrahedrons are the basic building blocks for various zeolite structures, such as zeolites A and X, the most common commercial adsorbents.

To prepare a suspension of zeolite, 3.0 g of zeolite type 3A powder in 20 ml MDF was mixed with 5.0 ml acrylonitrile polymer and refluxed for 1 h at 70 ℃. Then, 30.0 g of zeolite grains (mesh 3 to 6 mm) as the support were added to this mixture in 1.0 M NaOH solution. The prepared mixture was refluxed for 2 h and then centrifuged and dried out under nitrogen atmosphere at 400 ℃. At this
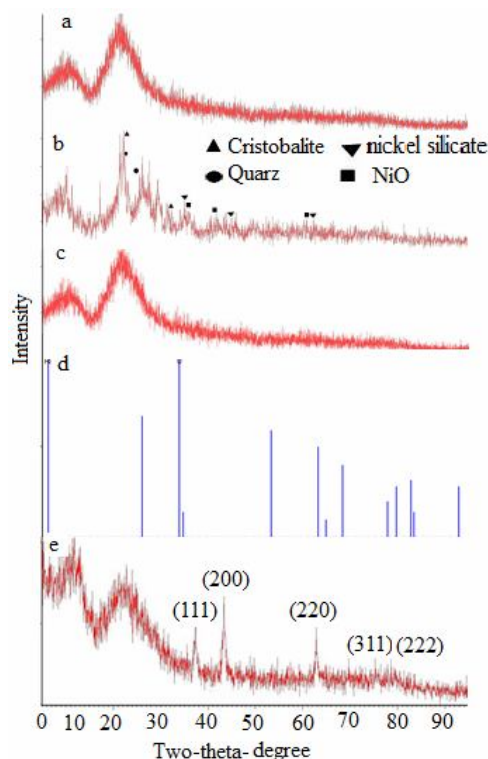

Fig. 3. The XRD patterns of silica particles in the absence of nickel (a), and the primary silica supported by nickel at 190 °C and heat treated at 600 °C (b), NiO/SiO_2 at 190 °C (c), the position of Ni(OH)2 in the c pattern (d) and post treatment NiO/SiO_2 by calcinig the obtained $Ni(OH)_2$ powder at 600 °C for 40 min (e).

stage a nanostructure ceramic form of the mixed matrix membranes (MMMs) were coated on the surface of zeolite grains. The nanostructure metallic nickel was deposited into the structure of the coated MMMs on the surface of zeolite particles by the electroless deposition technique [38]. I this study, the synthesized MMM-based catalyst was characterized by some microscopic and analytical methods such as SEM, XRD, IR, BET and BJH analysis. These analytical techniques were adopted for characterization of the synthesized catalyst from various aspects such as direct observation using the SEM imaging, physical studies (BET and BJH analysis) and spectroscopic investigations using XRD and IR spectrum.

The structure of the prepared deposited nickel on the

MMMs was characterized by FTIR spectra (Fig. 4), XRD pattern (Fig. 5), and SEM images (Fig. 6). As clearly shown in Fig. 4, observation of the significant shift in the SiO_2 stretching mode from 1002 cm^{-1} (Fig. 4a) to ~1458 cm^{-1} (Fig. 4b) clearly points out to the formation of the new morphology named MMMs [39]. Also, observation of the new absorption peak at ~462 cm^{-1} is related to the modification of the zeolite-based MMMs with Ni nanoparticles.

These results are also in good agreement with the XRD patterns (Fig. 5) during observation of partial shift in the diffraction peak of SiO_2 functional group at 2θ = ~30°. Also, modification of nickel nanoparticles on the surface of the zeolite-based MMMs is approved during observation of the weak peaks at 2θ equal to ~46, ~53 and ~78°, which points out to the applicability of the recommended procedure for modification of the zeolite-based MMMs with Ni nanoparticles. The reliability of these results is finally evaluated using direct observation of the synthesized catalyst (Ni-doped zeolite-based MMMs using SEM, Fig. 6) and also using the BET isotherms. According to the BET isotherm, the specific surface area of the prepared Ni on zeolite catalyst was found to be 31.5 m^2 g^{-1}. Mean pore diameter of the prepared Ni/zeolite catalyst from BJH method was found to be 10.88 nm.

Kinetics Tests

All the kinetics experiments were carried out in a flow system consisting of a one meter tabular quartz reactor similar to those used previously in this laboratory [40]. A specific amount of catalyst was placed in a 16.0 mm i.d. tabular quarts reactor where 43-cm-long section of the reactor was heated by a resistive furnace to be sure the catalyst and the feed gas is reached to the desired temperature. The reactor temperature was controlled by a platinum/platinum-13%-rhodium thermocouple. The pressure in the reactor and also the flow rate of the feed gas over the catalysts were controlled by BD/26.600G pressure transducer and two needle valves at the inlet and outlet of the reactor. To analyze the reaction mixture at the outlet of the reactor, two GCs with flame ionization detector (Shimadzu GC-8A) and thermal conductivity detector (PYE Unicam 204) along with 3 meter long silica gel columns were used. A six-way gas sampling valve along with a
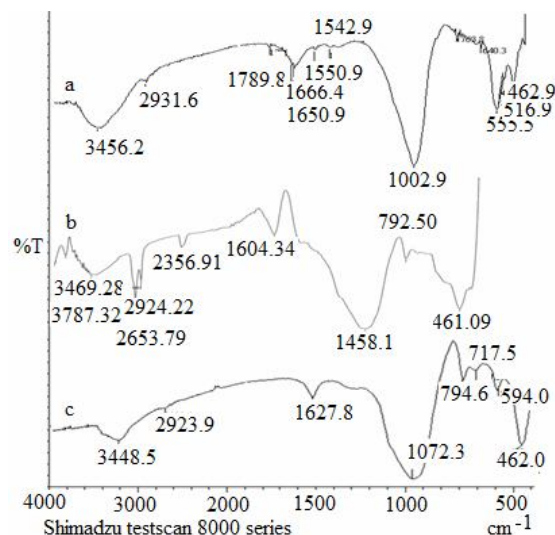

Fig. 4. FTIR spectra of zeolite 3A (a), zeolite-based MMMs (b), and nickel supported on the zeolite-based MMMs (c).

Fig. 5. The XRD pattern of natural zeolite (top) and nickel supported on zeolite-based MMMs (bottom).

3-cm^3 sampling loop was used to introduce the reaction mixture into the GCs for analyzing.

The experiments were performed under sub-atmospheric pressure and temperature range from 810 ± 10 K to 985 ± 10 K. The composition of the reaction mixtures at the outlet of the reactor chamber was compared with the composition of the feed gas at the inlet of the reactor (as the blank) to

Fig. 6. SEM images of surface of zeolite-based MMMs of nickel.
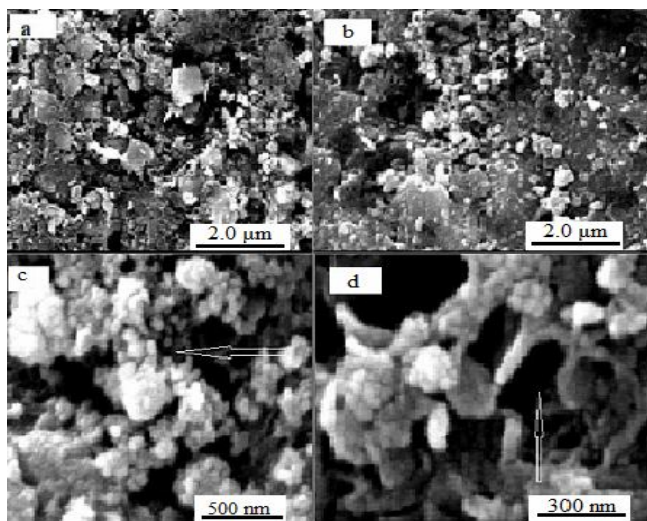
measure the feed gas conversion. Some experiments were carried out at the same conditions with no catalyst to test the efficiency of the prepared catalysts. Each experiment was repeated at least for three times and the magnitude of the error for each kinetics data is less than 10%.

ACTIVITY RESULTS

Kinetics experiments at different conditions were carried out to determine the efficiency of the prepared catalysts towards the conversion of feed gases. To examine the possible reactions on the surface of the reactor, two 100-cm-long cylindrical quartz reactors with different surface-to-volume ratios were used. The cross sections of the reactors were 2.76 and 5.27 cm^2. The surface-to-volume ratios (S/V) for these reactors were 4.5 and 2.4 cm^{-1}, respectively. Normally, the surface of the reactors after each experiment

Table 1. Conversion of Methane and Ethylene as Feed Gas in the Absence of any Catalyst in Two Reactors with Different Surface to Volume Ratio at Flow Rate of (25 ± 2) ml min^{-1}

Reactant	Feed Gas % Composition	Product % Composition	
Methane as feed gas at 950 ± 10 K and 350 ± 5 Torr, flow rate =			
		a*	b*
Methane	99.98	85.1 %8.6 ± 0.5 conversion	87.7 %6.9 ± 0.5 conversion
Ethane	0.0	0.0	0.0
Ethylene	0.0	0.0	0.0
Hydrogen	0.0	14.9	13
Ethylene as feed gas at 900 ± 10 K and 420 ± 5 Torr, flow rate =			
Methane	0.0	0.5	0.3
Ethane	0.0	0.3	0.6
Ethylene	99.90	71.3 17.8% conversion	68.9 19.7% conversion
Hydrogen	0.0	27.8	30.0

*S/V ratio of 2.4 cm^{-1} (**a**) and 4.5 cm^{-1} (**b**).

was being cleaned by passing hot air through the reactor. The results are shown in composition percentage by converting the concentration of each gaseous constituent at the outlet of the reactor.

The experiments with no catalyst were carried out at temperature range of 950 ± 10 K and 900 ± 10 K for methane and ethylene, respectively, in each of the two reactors to test for any possible surface reaction. In Table 1, the results of the conversion of the pure methane and ethylene as feed gases in the absence of any catalyst at temperatures of 950 ± 10 K and 900 ± 10 K and pressures of 350 ± 5 and 420 ± 5 Torr, respectively, are shown. As shown in Table 1, with clean quartz reactors at identical pressures, there was no trend evident on the conversion of feed gases by changing the surface-to-volume ratio of the reactor. The total conversion of methane and ethylene at these conditions was found to be 6.9% to 8.6%, and 17.8% to 19.7%, respectively. From the results shown in Table 1,

the conversion of methane to carbon and hydrogen on average was found to be about $8.0 \pm 1\%$ that completely converted to hydrogen and carbon. The results on the conversion of ethylene in Table 1 indicate less than 1 percent formation of methane and ethane, while from mass balance it was found that about $16 \pm 1\%$ of ethylene has been converted to carbon, hydrogen, and heavier hydrocarbons.

In some experiments, nickel metal in a honeycomb form was used as catalyst. In Table 2, the results of the methane conversion at 935 ± 10 K and 470 ± 5 Torr and 955 ± 10 K and 460 ± 5 Torr on the surface of honeycomb nickel are presented. Table 3 shows the results of the ethylene conversion at 900 ± 10 K and 415 ± 5 Torr and 870 ± 10 K and 355 ± 5 Torr on the surface of honeycomb nickel. As shown in Table 2, the conversion of methane into carbon and hydrogen on the surface of honeycomb nickel is increased by 15 to 21%, depending on the temperature and

Table 2. Conversion of Methane in the Presence of Honeycomb Nickel Catalyst, Mass of Catalyst: 6.3 ± 0.2 g

Reactant	Feed Gas % Composition	Product % Composition
T = 935 ± 10 K, P = 470 ± 5 Torr, Flow Rate = (33 ± 2) ml min^{-1}		
Methane	99.9	74.5 15.2% conversion
Ethane	0.0	0.0
Ethylene	0.0	0.0
Hydrogen	0.0	25.5
Hydrogen flow rate (ml min^{-1})		16.3
Carbon deposition mg min^{-1}		1.3
T = 955 ± 10 K, P = 460 ± 5 Torr, Flow Rate = (27 ± 2) ml min^{-1}		
Methane	99.9	65.0 21.8% conversion
Ethane	0.0	0.0
Ethylene	0.0	0.0
Hydrogen	0.0	35.0
Hydrogen flow rate (ml min^{-1})		13.8
Carbon deposition mg min^{-1}	0.0	1.1

flow rate, while the conversion of ethylene (Table 3) on this catalyst is increased from 97 to 98%, with about 13% formation of the methane and ethane in whole.

The results for the conversion of methane and ethylene on the surface of NiO/SiO_2 catalyst are shown in Tables 4 and 5, respectively. The conversion of methane to carbon and hydrogen on the surface of this catalyst reached to 35.7% at 930 K that completely converted into carbon and hydrogen, while the conversion of ethylene was found to be 92.4% at 850 K (*i.e.* 9.8% to methane and 2.9% to ethane and the rest to carbon, hydrogen, and heavier hydrocarbons). At lower temperature, 810 K, the conversion of ethylene was found to be just 68% that most of the converted ethylene transferred into methane and ethane (27.5% methane and 14.5% ethane).

Tables 6 and 7 show the results of the conversion of the methane and ethylene on the surface of nano-sized nickel coated on the zeolite grains using the MMMs method. The results indicate that the conversion of the methane to carbon and hydrogen on the surface of the Ni/zeolite is about

21.4%, while the conversion of the ethylene was found to be only about 14.1% that is mostly converted into the hydrogen and carbon.

DISCUSSION

The main purpose of the present study is to investigate the catalytic role of the tested catalysts on the dehydrogenation of methane. Natural gas consists of mainly methane and some ethane and ethylene in less extent. In this study, investigation of the ethylene conversion was interested just because of its presence in the composition of the natural gas. The conversion of ethane is not so crucial as conversion of ethylene in the natural gas stream.

CO_2-free production of hydrogen *via* thermo-catalytic decomposition of hydrocarbon fuels as a viable alternative to the conventional processes is the main objective in this paper.

Our kinetics results indicate the catalytic rule of those catalysts that tested in this study towards the conversion of

Table 3. Conversion of Ethylene Gas in the Presence of Honeycomb Nickel Catalyst. Mass of Catalyst: 6.7 ± 0.2 g

Reactant	Feed Gas % Composition	Product % Composition
T = 900 ± 10 K and P = 415 ± 5 Torr, Flow Rate: (33 ± 3) ml min^{-1}		
Methane	0.0	7.8
Ethane	0.0	5.3
Ethylene	99.9	2.1
		96.9% conversion
Hydrogen	0.0	84.8
Hydrogen flow rate (ml min^{-1})		42.5
Carbon deposition mg/min		6.9
T = 870 ± 10 K and P = 355 ± 5 Torr, Flow Rate: (20 ± 2) ml min^{-1}		
Methane	0.0	6.4
Ethane	0.0	6.8
Ethylene	99.9	1.2
		(98.0% conversion)
Hydrogen	0.0	87.6
Hydrogen flow rate (ml min^{-1})		26.5
Carbon deposition mg min^{-1}	0.0	4.3

Table 4. Conversion of Methane Gas in the Presence of NiO/SiO$_2$ at Two Different Conditions T = 930 ± 10 K, P = 490 ± 5 Torr, Flow Rate = (25 ± 2) ml min^{-1}, Mass of Catalyst = 3.5 ± 0.2 g

Reactant	Feed Gas % Composition	Product % Composition
Methane	99.9	48.2
		35.7 % conversion
Ethane	0.0	0.0
Ethylene	0.0	0.0
Hydrogen	0.0	51.8
Hydrogen flow rate (ml min^{-1})		28.8
Carbon deposition mg min^{-1}	0.0	2.3

Note: As shown, about 35 ± 2% carbon and heavier hydrocarbons were produced

T = 895 ± 10 K, P = 485 ± 5 Torr, Flow Rate = (27 ± 2) ml min^{-1}, Mass of Catalyst = 3.6 ± 0.2 g

Methane	99.9	66.1
		22.0 % conversion
Ethane	0.0	0.0
Ethylene	0.0	0.0
Hydrogen	0.0	33.9
Hydrogen flow rate (ml min^{-1})		18.8
Carbon deposition mg min^{-1}	0.0	1.5

Table 5. Conversion of Ethylene Gas in the Presence of NiO/SiO$_2$ at Two Different Conditions. T = 850 ± 10 K, P = 500 ± 5 Torr, Flow Rate = (33 ± 2) ml min^{-1}, Mass of Catalyst = 3.6 ± 0.2 g

Reactant	Feed Gas % Composition	% Product Composition
Methane	0.0	9.8
Ethane	0.0	2.9
Ethylene	99.9	4.6
		92.4 % conversion
Hydrogen	0.0	82.7
Hydrogen flow rate (ml min^{-1})		41.2
Carbon deposition mg/min	0.0	6.7

Note: As shown about 70 ± 2% carbon and heavier hydrocarbons were produced

T = 810 ± 10 K, P = 495 ± 5 Torr, Flow Rate = (30 ± 2) ml min^{-1}, Mass of Catalyst = 3.6 ± 0.2 g

Methane	0.0	27.5
Ethane	0.0	14.5
Ethylene	0.0	30.9
		68% conversion
Hydrogen	99.9	27.5
Hydrogen flow rate (ml min^{-1})		12.3
Carbon deposition mg min^{-1}	0.0	2.0

Table 6. Conversion of Methane Gas in the Presence of Ni/zeolite at 985 ± 10 K and 420 ± 5 Torr, Flow rate = (20 ± 2) ml min^{-1}, Mass of Catalyst = 6.2 ± 0.2 g

Reactant	Feed Gas % Composition	Product % Composition
Methane	99.9 4.2×10^{-5}	66.2 21.4% conversion
Ethane	0.0	0.0
Ethylene	0.0	0.0
Hydrogen	0.0	33.8
Hydrogen flow rate (ml min^{-1})		13.8
Carbon deposition mg min^{-1}	0.0	1.1

Table 7. Conversion of Ethylene Gas on the Surface of Ni/zeolite at 840 ± 10 K and 410 ± 5 Torr, Flow Rate = (20 ± 2) ml min^{-1}, Mass of Catalyst = 6.3 ± 0.2 g

Reactant	Feed Gas % Composition	Product % Composition
Methane	0.0	0.1
Ethane	0.0	0.1
Ethylene	99.9	75.2 14.1 % conversion
Hydrogen	0.0	23.9
Hydrogen flow rate (ml min^{-1})		4.3
Carbon deposition mg min^{-1}	0.0	0.7

methane obeys the following order, NiO/SiO$_2$ > Honeycomb nickel ≈ Ni/zeolite. In the present study, our results indicate 35.7% conversion of methane on the surface of NiO/SiO$_2$ with 4.5 to 5 weight percent of nickel according to ICP results. Our results could be compared with 45% methane conversion at 823 K reported by Couttenye et al. [24] on the surface of pure Ni and NiO, or 21% of methane conversion at 1050 K on the surface of Ca-Ni/TiO$_2$ reported by Hu, et al. [7], or %45 methane conversion in a 4.67 mol m^{-3} concentration of methane on the surface of nickel gauze at 773 K reported by Monnerat, et al. [25], or 30% of methane conversion on the surface of Ni/SiO$_2$ catalyst with 15% of Ni at 923 K in a successive cracking cycles reported by Aiello et al. [26].

The effect of temperature is tested on the activity of the NiO/SiO$_2$ and Honeycomb nickel catalyst. As shown in Table 2, increasing the temperature of the reactor from 935 K to 955 K and flow rate from 27 ml min^{-1} to 33 ml min^{-1} causes a 30 percent increase on the rate of conversion of methane on the surface of honeycomb nickel catalyst, while increasing the temperature from 870 K to 900 K and flow rate from 20 ml min^{-1} to 33 ml min^{-1} (Table 3) does not change the amount of conversion of ethylene on the surface of honeycomb nickel catalyst just because, the increase of temperature causes an increase on the rate but increase of the flow rate causes a decrease on the rate of conversion.

In Table 4, increasing the temperature from 895 K to 930 K causes 38 percent increase on the rate of conversion of methane on the surface of NiO/SiO$_2$, with almost the same flow rate. Increasing temperature from 810 K to 850 K

causes a 36 percent increase on the rate of conversion of ethylene on the surface of NiO/SiO_2, Table 5, with almost the same flow rate.

Comparing the data in Table 3 and Table 5, indicates that the methane selectivity (formation of methane) on the surface of NiO/SiO_2 is much higher than that on the surface of honeycomb nickel for the conversion of ethylene.

In Tables 2-5, the deposited amount of carbon is reported based on the carbon balance with 10% error. The density, flow rate, and conversion percentage of the feed gases are used to calculate the rate of deposition of carbon (in mg min^{-1} unit) on the surface of catalysts beside the inner surface of the reactor.

Carbon buildup is one of the major issues in the conversion of methane to hydrogen regardless of the methods used. Normally, the carbon is forming continuously during the experiment and depositing anywhere especially on the surface of the catalyst. Deposition of the carbon on the surface of the catalyst causes deactivation of the catalyst. It has been noticed that the activity of the catalysts decreases after each experiment. The durability of the NiO/SiO_2 towards the conversion of methane was tested for 15 h. Its activity towards conversion of methane decreased by 10% as shown in Fig. 7. It was possible to remove the coke from the surface of the catalyst and inner surface of the reactor by passing the hot air (550 °C) inside the reactor for 30 min.

As shown in Tables 2 to 5, generally the concentration of hydrogen increases as flow rate decreases, but the flow rate of hydrogen decreases as feed gas flow rate decreases that is due to the shortage of the amount of methane or ethylene that enter into the reactor at lower flow rates. The hydrogen flow rate is calculated from the corresponding rate of carbon deposition.

CONCLUSIONS

The Kinetics tests indicate the prepared NiO/SiO_2 catalyst has a better efficiency on the conversion of methane, up to 35.7% at temperatures below 1000 K. The nano-scale nickel catalyst coated on the surface of zeolite particles using MMMs method as interface caused the conversion of methane to reach to 21.4%. The advantage of these kinds of membranes is their nanostructure porosities. It seems that the lower activity of the Ni/zeolite catalyst
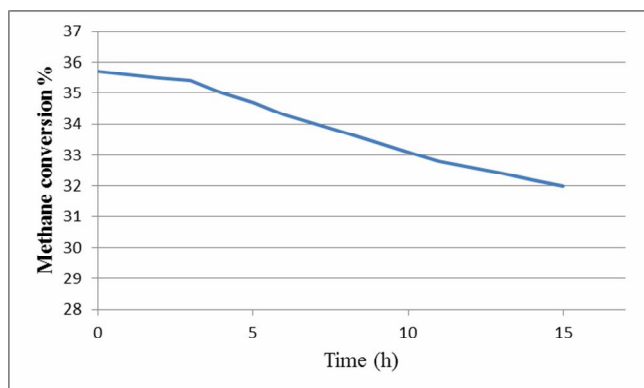
Fig. 7. Performance of the NiO/SiO_2 catalyst as a function of time. Flow rate = 35 ml min^{-1} at 920 K and 420 Torr pressure.

relative to NiO/SiO_2 catalyst is due to its smaller specific surface area (about 31.5 m^2 g^{-1}) relative to that of NiO/SiO_2 (221 to 273.8 m^2 g^{-1}). The results indicate that the conversion of the ethylene into methane, ethane, carbon, hydrogen and in some extend heavier hydrocarbons is occurred, while methane is just converted to hydrogen and carbon in agreement with reported results by Couttenye *et al*. [24]. When ethylene is used as the feed gas, the selectivity of NiO/SiO_2 catalyst towards the formation of methane is about 3 times greater than that for honeycomb Ni catalyst and much higher than that for Ni/zeolite catalyst.

ACKNOWLEDGMENTS

REFERENCES

[1]   EPA United States Environmental Protection Agency, http://www.epa.gov/climatechange /ghgemissions/gases.html, Accessed on, 2014.

[2]   P. Nema, S. Nema, P. Roy, J. Renewable and Sustainable Energy Reviews (J.RSER) 16 (2012) 2329.

[3]   K.E. Parent, Fuel Cells, 2003 Theme: Earth's Atmosphere and Beyond.

[4]   H. Shuanghui, W. Baowei, L. Yijun, Y. Wenjuan, Plasma Sci. Technol. 15 (2013) 555. T. Kolb, J.H. Voigt, K..-H. Gericke, Plasma Chem. Plasma Process 33 (2013) 631. B. Wang, W. Yan, W. Ge, X. Duan, J. Energy Chem. 22 (2013) 876. Q. Liu, H. Zheng, F. Pan, G. Pan, R. Yang, ASME 2013 Power Conference, Boston, Massachusetts, USA, July 29-August 1.

[5]   T. Boutot, Z. Liu, T.K. Whidden, Y. Yang, Procc. Hydrogen and Fuel Cells, 2007.

[6]   J.R. Rostrup-Nielsen, J. Sehested, J.K. Norskov, Adv. Catal. 47 (2002) 65.

[7]   C. Hu, H. Zhang, J. Wu, Pap.Am. Chem. Soc., Div. Fuel Chem. 49 (2004) 124.

[8]   K. Supat, S. Chavadej, L. Lance, L.L. Lobban, R.G. Mallinson, Fuel Chemistry Division Preprints 47 (2002) 269.

[9]   Y. Chen, Y. Wang, H. Xu, G. Xiong, Appl. Catal. B-Environ. 80 (2008) 283.

[10]   L.S. Neiva, L. Gama, Brazilian Journal of Petroleum and Gas 4 (2010) 119.

[11]   A.M. Gadalla, B. Bower, Chem. Eng. Sci. 43 (1988) 3049. M.C.J. Bradford, M.A. Vannice (1996). Appl. Catal. A 142 (1996) 73.

[12]   J.R. Rostrup-Nielsen, in: J.R. Rostrup-Nielsen. M. Boudart (Eds.), Catalysis-Science and Technology, Springer, Berlin, 1984, Vol. 5, p. 1. Rostrup-Nielsen, J.R. (1984a). Sulfur-passivated nickel catalysts for carbon-free steam reforming of methane, J. Catal. 85 (1984a) 31.

[13]   Q. Zhuang, Y. Qin, L. Chang, Appl. Catal. 70 (1991) 1.

[14]   V.R. Choudhary, B.S. Uphade, A.S. Mamman, Appl. Catal. A 168 (1998) 33.

[15]   T. Horiuchi, K. Sakuma, T. Fukui, Y. Kubo, T. Osaki, T. Mori, Appl. Catal. A 144 (1996) 111. T. Borowiecki, A. Golebiowski, B. Stasinska, Appl. Catal. A 153 (1997) 141.

[16]   M.A. Gerber, U.S. Department of Energy, PNNL-16950.

[17]   T.V. Choudhary, E. Aksoylu, D.W. Goodman, Catal. Rev. 45 (2003) 151.

[18]   J.R. Rostrup-Nielsen, J.H. Bak-Hansen, J. Catal. 144 (1993) 38.

[19]   D.L. Trimm, Catal. Today 37 (1997) 233.

[20]   Y. Chen, Y. Wang, H. Xu, G. Xiong, Appl. Catal. B-Environ. 80 (2008) 283.

[21]   N. Muradov, Proceeding of 2000 Hydrogen Program Review, NREL/CP-570-28890.

[22]   J.-L. Zeng, Z.-T. Xiong, H.B. Zhang, G.D. Lin, K.R. Tsai, Catal. Lett. 53 (1998) 119.

[23]   J.H. Lunsford, Catalysis Today 63 (2000) 165.

[24]   R.A. Couttenye, M. Hoz de Vila, S.L. Suib, Prepr. Pap.-Am. Chem. Soc., Div. Fuel Chem. 48 (2003) 799.

[25]   B. Monnerat, L. Kiwi-Minsker, A. Renken, Chem. Eng. Sci. 56 (2001) 633.

[26]   R. Aiello, J.E. Fiscus, H.-C. Zur Loye, M.D. Amiridis, Appl. Cat. A: General 192 (2000) 227.

[27]   Nano Poshesh Felez Company, http://www. nanochem.ir. 2014, Accessed on.

[28]   Determination of the Specific Surface Area of Solids by Gas Adsorption-BET Method. Second Edition of ISO 9277, ISO, Geneva, 2010.

[29]   E.P. Barrett, L.G. Joyner, P.P. Halenda, J. Am. Chem. Soc. 73 (1951) 373.

[30]   J. Chrusciel, L. Slusarski, Mater. Sci. 21 (2003) 461.

[31]   Y.D. Zhong, X.B. Zhao, G.S. Cao, J.P. Tu, T.J. Zhu, J. Alloys Compd. 420 (2006) 298.

[32]   P. Oliva, J. Leonardi, J.F. Laurent, C. Delmas, J.J. Braconnier, M. Figlarz, F. Fievet, A. de Guibert, J. Power Sources 8 (1982) 229.

[33]   S.V. Ganachari, R. Ravishankar Bhat, R. Raghunandan Deshpande, A. Venkataraman, Recent Research in Science and Technology 4 (2012) 50.

[34]   S.M. Hu, J. Appl. Phys. 51 (1980) 5945.

[35]   L.-T. Zhang, W.-F. Xie, et al. Chin. Phys. Latt. 20 (2003) 1366.

[36]   A. Bahari, D. Shajari, S. Khodadad, Int. J. Electrochem. Sci. 8 (2013) 9338.

[37]   L.A. Saghatforoush, M. Hasanzadeh, S. Sanati, R. Mehdizadeh, Bull. Korean Chem. Soc. 33 (2012) 2613.

[38]   J. Sudagara, J. Lianb, W. Sha, J. Alloys Comp. 571 (2013) 183.

[39]   Z. Haruna, M.F. Shohura, M.R. Jamalludina, M.Z. Yunosa, H. Basric, J. Teknologi 70 (2014) 15.

[40]   S.H. Mousavipour, V. Saheb, F. Pirhadi, M.R. Dehbozorgi, J. Iran. Chem. Soc. 4 (2007) 279.